Nat Hazards (2015) 76:347–372
DOI 10.1007/s11069-014-1493-9

ORIGINAL PAPER

Flood risk modeling for optimal rice planning for delta region of Mahanadi river basin in India

Dibyendu Samantaray · Chandranath Chatterjee · Rajendra Singh · Praveen Kumar Gupta · Sushma Panigrahy

Received: 25 March 2014 / Accepted: 28 October 2014 / Published online: 11 November 2014

Abstract Flood risk management serves to reduce the negative consequences of flood disaster to a certain extent. In agriculture-dominated countries, the extent of damage incurred in crop land by heavy and frequent floods is quite high. The present study aims to develop an optimal rice planning procedure considering the flood risk through hydrodynamic floodplain modeling in flood-prone delta region of Mahanadi river basin in India. As high-resolution topographic data and surveyed river cross sections are unavailable for the study area, MIKE FLOOD model setup is prepared using river cross sections and floodplain elevation model derived from freely available SRTM DEM. In this study, MIKE FLOOD setup is prepared and flood inundation simulation is carried out. Flood inundation extent obtained is compared with RADARSAT-1 image-based inundation extent. Subsequently, flood risk is evaluated for cropping pattern in floodplains using functional relationships between flood characteristics and the expected damage of different rice varieties. Based on the flood risk, an optimal rice planning model is developed for maximizing the net benefits in the floodplain. The average annual expected net benefit of optimal rice allocation model for the study area is to the tune of INR 601 million compared to INR 432 million for normal rice variety cultivation throughout the study area.

Keywords Mahanadi delta · MIKE FLOOD · Flood risk assessment · RADARSAT · Optimal rice planning

D. Samantaray · C. Chatterjee (✉) · R. Singh
Agricultural and Food Engineering Department, Indian Institute of Technology, Kharagpur 721302, India
e-mail: cchatterjee@agfe.iitkgp.ernet.in

P. K. Gupta · S. Panigrahy
Space Applications Centre, Indian Space Research Organisation, Ahmedabad 380015, India

1 Introduction

Floods are one of the most recurring and frequent natural catastrophes experienced by mankind since time immemorial. Flooding and flash flooding poses serious hazards to economy, population and environment in many parts of the world. According to the Federal Emergency Management Agency (FEMA) of the United States, floods are the second most common and widespread of all natural disasters. In India, the area affected from floods is on an average 4.942 million hectare from the year 2000–2009. During this period, the monetary damage to the tune of Indian rupees (INR) 36,004.75 million (Central Water Commission 2010) is observed. Intense rainfalls in monsoon season (June–September), drainage congestion leading to water-logging problem and low carrying capacity of river channels trigger frequent flooding in the delta and coastal areas of India (NDMA 2008). Despite the fact that the river channels in these areas are protected through embankments, low carrying capacity of the channels leads to bank spill over and breaching. Consequently, flooding in these areas is aggravated.

In developing countries such as India, the trend of destruction due to flood is increasing significantly due to severe intrusion into the floodplains for urbanization and agriculture. Increasing frequency of flood events without proper flood management strategies is triggering heavy losses. In India, on an average 4.048 million hectare crop area was damaged due to flood in the period 2000–2009 (Central Water Commission 2010). The monetary loss due to crop damage incurred in this period is to the tune of INR 11,077.75 million (Central Water Commission 2010). In India, the available flood management strategies in agricultural lands are through structural measures and rescheduling of cropping pattern in the affected areas. As these strategies are not effective in long term, a comprehensive study to plan the cropping pattern in flood-affected crop lands taking flood risk into account is of utmost need.

As this kind of disaster cannot be prevented or regulated, precautionary management practices based on scientific and historical knowledge are most effective methods to minimize the losses. In recent years, floodplain management extended beyond conventional (structural) measures involving scientific knowledge and practice to reduce risks and impacts (Burrel et al. 2007). Flood risk mapping, flood hazard mapping, floodplain zoning and flood forecasting are playing important roles in assessing the current trend and future scenarios of flood risk. In flood hazard assessment, the flood events are characterized by spatio-temporal characteristics (extent of areal inundation, inundation depth, inundation duration, flow velocity, etc.) and associated recurrence interval/return period. Flood risk is assessed by integrating vulnerability of the elements at risk and flood hazard (Mileti 1999; Dang et al. 2011).

Quantification of parameters such as flood depth, inundation extent, inundation duration and flow velocity which contribute to the damaging potential of a flood event requires use of flood inundation models based on advanced algorithm and high-quality input data. In developing countries such as India, unavailability of precise and high-quality input data restrict the use of flood inundation models (Sanyal and Lu 2004; UNFCCC 2007). Therefore, to derive flood inundation extent, satellite remote sensing and GIS techniques are widely used in developing countries. Till date, satellite remote sensing has become a practical tool for development of cost-effective methods to monitor the spatial extent of flooding. However, the limitation of the satellite remote sensing includes inability to provide information regarding spatio-temporal characteristics of other parameters such as flood depth and flow velocity. As flood hazard management essentially requires the spatio-temporal characteristics of these parameters, recent advances in satellite remote sensing

and GIS techniques can play an important role in extracting the required input topographic data for flood inundation model setup (Bates et al. 2003; Werner 2004; Haile and Rientjes 2005; Sanders 2007; Tarekegn et al. 2010; Khan et al. 2011).

Geometric description of river bathymetry (channel geometry and longitudinal slope of riverbed) and continuous surface representation of the floodplain (digital elevation model) are the important inputs to flood inundation models (Nicholas and Walling 1997). Patro et al. (2009b) and Pramanik et al. (2010) have used Shuttle Radar Topography Mission (SRTM) digital elevation model (DEM) to extract river cross sections for MIKE 11 hydrodynamic model setup. Tarekegn et al. (2010) have used Advanced Spaceborne Thermal and Reflection Radiometer (ASTER) data to create 15 m resolution DEM for two-dimensional hydrodynamic flood modeling. Wang et al. (2012) have concluded that SRTM and ASTER DEM can be beneficial in hydraulic modeling for data scarce condition where high-resolution DEMs are not available. Additionally, flood inundation extent output from flood inundation models can be effectively validated using flood inundation extent derived from satellite remote sensing data (Aronica et al. 2002; Horritt 2006). Satellites carrying synthetic aperture radar (SAR) sensors are particularly gaining popularity over optical sensors for flood inundation extent extraction due to their cloud penetrative ability. Several researchers have effectively used SAR data from European Remote Sensing (ERS), RADARSAT, TerraSAR-X and COSMO SkyMed for flood extent mapping (Long and Trong 2001; Bazi et al. 2005; Waisurasingha et al. 2008; Di Baldassarre et al. 2009; Schumann et al. 2009, 2010; Matgen et al. 2011).

Recently, use of hybrid models (one-dimensional hydrodynamic river model linked to two-dimensional hydrodynamic floodplain model) in floodplain inundation modeling is gaining popularity due to less computational effort compared to full two-dimensional models (Bates and De Roo 2000; Villanueva and Wright 2006). MIKE FLOOD is a hybrid model developed at Danish Hydraulic Institute which dynamically integrates MIKE-21 (two-dimensional) and MIKE-11 (one-dimensional) models in a single environment (DHI 2004). Several researchers have demonstrated the practical applicability of MIKE FLOOD model (Kjelds and Rungo 2002; Rungo and Olesen 2003; Chatterjee et al. 2008; Patro et al. 2009a; Vanderkimpen et al. 2009; Mani et al. 2014).

Vulnerability analysis focuses on estimating the damaging effect of the hazard on the exposed elements. Frequently, vulnerability analysis focuses on direct flood loss in monetary terms using damage functions (Thieken et al. 2008). Damage functions are generated through coupling the values of inundation with degree of damage; hence, they enable to characterize the direct effect of floodwater on different types of exposed elements. Such functions are the essential building blocks for flood loss estimation (Forster et al. 2008b; Bouwer et al. 2009; Luino et al. 2009). Several loss functions are developed including the parameters like flow depth, flow velocity, inundation duration, time of occurrence, etc. (Penning-Rowsell and Tunstall 1996; Buchele et al. 2006). Approaches for the estimation of agriculture product damages are established through damage to arable land (crops) and grassland (Hoes and Schuurmans 2006); and damage to several crop types (Dutta et al. 2003; Forster et al. 2008b).

Considering the above facts, we have tried to setup MIKE FLOOD model using SRTM DEM-extracted topographic data for delta region of Mahanadi river basin, Odisha, India. Subsequently, the model setup is used for flood hazard mapping of the study area. An optimal rice planning model through flood risk analysis is developed for the study area in order to maximize the net benefit while minimizing the flood losses. The proposed rice planning methodology is expected to be unique of its kind as rice planning strategy which takes into account flood risk is yet to be reported globally.

The structure of this paper is as follows: Sect. 2 presents the study area description; Sect. 3 gives the details of the data used in this study; Sect. 4 explains the complete methodology followed in this study; Sect. 5 contains the results obtained in this study and a critical discussion on the results; and Sect. 6 summarizes the conclusions.

2 Study area

Delta region of Mahanadi river basin is selected as the study area, which is located in the northeastern part of coastal Orissa, India, between the longitudes 85° 30′E and 86° 52′E and the latitudes 19° 40′N and 20° 45′N. Kathajodi is the major distributary of river Mahanadi at Naraj which is around 500 m downstream of the delta head Mundali. The other distributaries of river Mahanadi are Birupa, Chitroptala, Paika and Luna. Kuakhai, Biluakhai, Kandal and Devi are the distributaries of river Kathajodi. Kushabhadra and Bhargabi are the distributaries of river Kuakhai. River Daya has two distributaries named Rajua and Makara. All the rivers fall into Bay of Bengal except Daya and Bhargavi which fall into Chilika Lake. The orientation of the rivers forms 4 major doabs in the delta region. The areal extent of the delta is about 9,063 km^2.

In a span of 52 years (1960–2011), the delta region has experienced flood about 23 times (SRC 2011–2012). The most recent flood years are 2006, 2007, 2008, 2009 and 2011. The delta region accounts for around 57 % of total crop area affected due to flood in Orissa in 2011, 22 % of total crop area affected due to flood in Orissa in 2009 and 53 % of total crop area affected due to flood in Orissa in 2006. Due to floods, more than 50 % of the Kharif season (June–December) crop-loss is estimated in some parts of this region (SRC 2008–2009). The main reason behind frequent floods in this region is heavy precipitation in the upstream area of delta region and low carrying capacity of the river channels. Historic flood events in Mahanadi delta (1960–2011) show that 69 % major floods are due to the contribution from uncontrolled catchment above the delta head Mundali (Parhi et al. 2012). Presence of low-level escapes in the rivers to allow some portion of peak flows into the floodplain, and multiple breaching locations aggravate the flooding scenarios in this region (Khatua and Patra 2004). Rice predominates the cropping pattern in this coastal region, making it virtually a monoculture region. The details of the geographical location of Mahanadi delta region are given in Fig. 1.

3 Data used

The data used in this study are the river cross sections, time series of discharge or water level or both, rainfall data, embankment data, data on different structures, topographical map, SRTM DEM, RADARSAT-1 images for the entire study area and flood damage data. Table 1 summarizes the data used in this study. The river cross sections, time series of discharge or water level or both, embankment data, data on different structures, and topographical map data are collected from Orissa State Water Resources Department (SWRD), Cuttack; State Surface Water Data Center (SSWDC), Bhubaneswar; Central Water Commission (CWC), Bhubaneswar. Details of different rice varieties used in Kharif season are collected from Central Rice Research Institute (CRRI), Cuttack (Progress Report: Vol 1 DRR 2008); Directorate of Water Management (DWM), Bhubaneswar; Orissa University of Agriculture and Technology (OUAT), Bhubaneswar (Shuttle breeding report 2008); Directorate of Agriculture and Food Production (DAFP), Bhubaneswar; and

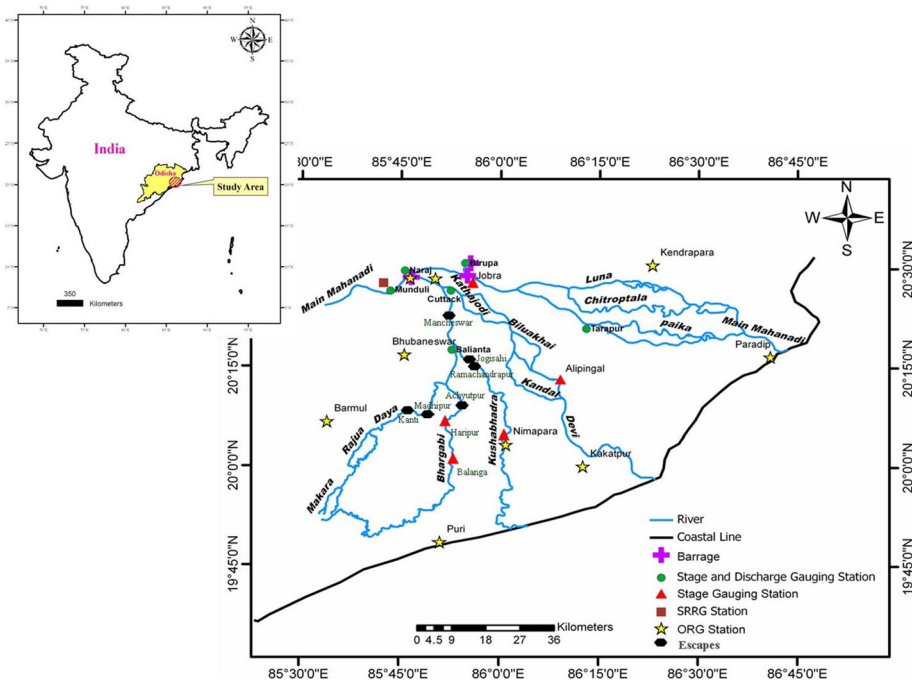

Fig. 1 Index map of delta region of Mahanadi river basin

Orissa Space Application Centre (ORSAC), Bhubaneswar. Several experimental data such as yield comparison of submerged rice variety with parent varieties; deep water varieties and their yield compared with local varieties; and shallow water varieties and their yield compared with local varieties are also collected. RADARSAT-1 images of 20th July, 13th August and 6th September for the year 2001; and 4th September for the year 2006 are obtained from Space Application Centre (SAC), Ahmedabad.

4 Methodology

4.1 Flood inundation mapping using MIKE FLOOD

In MIKE FLOOD simulation, both MIKE 11 and MIKE 21 model setups are required in order to dynamically link them. The MIKE 11 model setup is prepared to represent the entire river system in the delta region. There are thirteen open hydrodynamic boundaries. All boundaries are provided with constant water levels except at two points, i.e., the upstream boundary at Mundali, where 3-hourly discharge data are provided and the boundary at the upstream of Birupa barrage on the river Birupa is given as daily water level time series data. As very few measured river cross sections are available, SRTM DEM-extracted cross sections are used along with the measured ones. The details of the procedure used to extract and refine the cross sections are discussed in Patro et al. (2009b). The MIKE 11 model is calibrated for flooded year and validated for different non-flooded years. Initially, during calibration, the Manning's n values are taken from literature (Chow 1959)

Table 1 Details of different data used in the study

Type of data		Data period (year)	Purpose of use
Survey of India topomaps			Base map preparation
Drainage network, embankment details and structural details of escapes			Model input
Satellite remote sensing data			
RADARSAT-1		2001 and 2006	Flood inundation mapping and rice mapping
SRTM			Cross-section extraction and floodplain representation
Hydrological data			
Station name	Data interval		
Discharge-water level			
Mundali and Birupa	3 hourly	2001–2004 and 2006	Model input
Naraj, Cuttack, Balianta and Tarapur	Daily	2002–2004	MIKE 11 model calibration and validation
Madipur, Kanti, Jogisahi, Ramachandrapur and Achyutpur	Hourly	2003	MIKE 11 model calibration and validation
Water level			
Naraj, Balianta, Cuttack, Tarapur, Nimapara and Alipingal	Hourly	2002–2004	MIKE 11 model calibration and validation
Rainfall data			
Station name	Data interval		
Puri, Nimapara, Bhubaneswar, Kakatpur, Barmul, Paradip, Kendrapara, Cuttack and Naraj	Daily	2001 and 2006	MIKE 21 model input
Crop related data			
Experimental data on effect of submergence and performance of different rice varieties			Stage-duration-damage function and optimal crop planning

which is then modified subsequently. During the process of calibration and validation, model performance is assessed for different gauging sites present in the area using different performance indices like root mean square error (RMSE), mean absolute error (MAE), coefficient of determination (R^2), index of agreement (d), absolute deviation in peak and percentage deviation in peak. For flood inundation simulation, the calibrated MIKE 11 model is coupled with MIKE 21 model using MIKE FLOOD for the monsoon period of the flooded years. The MIKE 21 model contains information regarding the elevations of the floodplain, rainfall at different locations and the Manning's n values for the floodplain.

4.2 Flood inundation mapping with GIS and remote sensing data

Dependence of optical sensors on cloud conditions restricts their use in flood monitoring. Radar data are therefore often more suited in flood inundation monitoring in cloudy

conditions. In this study, RADARSAT-1 images are used for flood inundation mapping. Gray level thresholding and visual interpretation techniques are carried out to find inundated areas. Subsequently, regular water bodies are eliminated to obtain actual flood inundation area. Additionally, rice mapping is carried out to separate rice-transplanted area having standing water and actual flooded area in the RADARSAT-1 images corresponding to flood dates coinciding with the normal rice transplanting period of the study area. Rice area mapping and regular water body mapping procedures are discussed in following sections.

4.2.1 Rice area estimation

Rice area is mapped for the study area by modifying the rice mapping methodology proposed by Chaoudhury and Chakraborty (2006). According to the methodology, rice area is estimated on the basis of temporal variation of backscatter coefficients of rice fields. The analysis of the backscatter coefficient of rice crop shows significant temporal behavior during its growth period due to the interaction of microwave radiation with the crop canopy increasing from the transplanting stage to the reproductive stage. This temporal variation of backscatter coefficients clearly differentiates rice fields from other land-cover classes.

Knowledge-based decision rule classifier is used to classify rice and non-rice areas. The first date is acquired coinciding with the puddling/transplanting stage. The other two dates are acquired at 24-day interval, which covered growth until the peak vegetative stage of the crop. The three-date data are stacked into single multi-temporal layer, which reflects the variation in rice planting of the study area. The stacked image is then assigned the primary colors of red, green and blue to generate multi-temporal RADARSAT false color composite (FCC) image. The first date (D1), second date (D2) and third date (D3) RADARSAT-1 images are assigned to red (R, i.e., channel 1), green (G, i.e., channel 2) and blue (B, i.e., channel 3), respectively. Difference images of different dates are prepared for further use in the analysis. Here, the decision rules developed for classification of rice subclass areas are:

If $[-18.5 \leq dB_{D1} \leq -11]$ and $[(dB_{D2}-dB_{D1}) \geq 2]$ and $[(dB_{D3}-dB_{D2}) \geq 2]$ and $[-11 \leq dB_{D3} \leq -5]$, then assign the pixel as normal sown rice (cyan and blue color in the multi-temporal RADARSAT FCC image). dB_{D1} represents the backscatter values of first date RADARSAT-1 image. Similarly, dB_{D2} and dB_{D3} represent the backscatter values of second and third date RADARSAT-1 images, respectively.

4.2.2 Estimation of regular water bodies

Backscatter values of July 20, 2001 and September 4, 2006, for river area are found to be less than −17 dB. Thus, for regular water body identification −17 dB is used as threshold value. Due to specular reflection, these areas are found to be dark in tone. However, increase in backscatter values is observed for water bodies having different textured material such as vegetation, sediment and settlements. Wet lands also have higher backscatter values. Therefore, backscatter value of −17 dB is used in following logical operations to identify the regular water bodies in the study area.

A. $(dB_{D1} < -17)$ and $(dB_{D2} < -17)$ and $(dB_{D3} < -17)$
This implies that water is present in all three dates.

B. ($dB_{D1} > -17$) and ($dB_{D2} < -17$) and ($dB_{D3} < -17$)
This implies water is not present in first date, but second and third dates have water.
C. ($dB_{D1} < -17$) and ($dB_{D2} < -17$) and ($dB_{D3} > -17$)

This implies water is present in first and second dates, but third date does not have water.

4.3 Validation of inundation map prepared using MIKE FLOOD

The performance of MIKE FLOOD model is assessed by comparing the inundated area (IA) derived from the RADARSAT data (IA_{obs}), with the inundated area predicted by the model (IA_{mod}). Deriving appropriate areal statistics is not straight forward; however, one possible measure of fit (Bates and De Roo 2000) is given by:

$$\text{Fit}\,(\%) = \frac{IA_{obs} \cap IA_{mod}}{IA_{obs} \cup IA_{mod}} \times 100 \quad (1)$$

This measure is equal to 100 % when the two areas coincide, and penalizes over- and under-prediction of inundated areas by the model.

4.4 Flood hazard assessment

L-moment based at-site flood frequency analysis (Hosking 1990; Kumar and Chatterjee 2005; Yang et al. 2010) is carried out to estimate the flood peaks of return periods 2, 10, 25, 50 and 100 years for Naraj gauging site of the study area. The flood hydrograph shape is obtained through a non-dimensional analysis of the peak flood hydrographs at Naraj gauging site (Forster et al. 2008a). The widest non-dimensional hydrograph, being the most potential to produce worst flood scenario, is selected to generate the flood hydrographs of different return periods. Each discharge ordinate of the widest non-dimensional hydrograph is multiplied by the flood value corresponding to a particular return period. This transformation yields the widest flood hydrograph corresponding to that return period. Thus, all the desired return period flood hydrographs are generated by combining the flood frequency analysis and non-dimensional flood hydrograph analysis. Subsequently, these flood hydrographs are used as upstream boundary condition in the calibrated MIKE 11 model setup; and flood hazard maps are generated using MIKE FLOOD model.

4.5 Flood vulnerability assessment

The selected rice varieties and their characteristics are shown in Table 2. Depth–duration–damage relationship for the rice varieties are summarized from the experimental data mentioned in Sect. 3 (Table 3). Subsequently, the monetary losses estimated using these functional relationships are used as the basic input in the rice planning model.

4.6 Development of optimal rice planning model

In this study, normal rice, shallow rice, medium deep rice, deep rice and submerged rice varieties are used. Net benefit for each rice variety is estimated by subtracting production cost from gross return. Gross return is calculated using product of yield, market price and recovery factor. Recovery factor is calculated using depth–duration–damage relationship derived from crop data. Expected annual net benefit is estimated using methodology

detailed in Kazama et al. (2009). Allocation of crop is determined on the basis of maximum sum of average annual expected net benefit from different return period floods in an area in the floodplain.

Average annual expected net benefit is calculated using product of interval average net benefit and interval probability. Interval average net benefit is estimated from net benefit associated with two return periods. Allocation of different rice varieties is carried out on the basis of maximum sum of expected annual net benefit for 5, 10, 25, 50 and 100 year return periods in respective areas of the floodplain.

In order to execute the above operation, an algorithm is developed and a computer program is written in C language. The 3 × 3 neighborhood clustering operation is carried out on the output obtained from C program to get the final rice allocation map. Flow chart showing detailed methodology of optimal rice planning is given in Fig. 2.

The following assumptions are made for optimal rice planning: (1) flooding occurs once in the growing season of the crop; (2) flooding occurs during the vegetative growth stage of the crop; (3) all rice varieties have same minimum cultivation cost; (4) submerged rice variety is allocated when depth of flooding is more than 2 m in every flooding.

5 Results and discussion

5.1 Flood inundation mapping using MIKE FLOOD

In this study, MIKE 11 model is calibrated for the year 2003 and validated for the years 2002 and 2004 after incorporating all the six river escapes namely Achyutpur, Jogisahi, Kanti, Madhipur, Mancheswar and Ramachandrapur in the MIKE 11 river network. These river escapes are responsible for a good amount of flooding in the downstream areas of the Kuakhai-Bhargabi-Daya river system as their main function is to spill out flood water into the adjacent floodplain. Flood year 2003 is selected as the calibration year in this study as during non-flooded years, the escapes remain dormant. Subsequently, the results of the MIKE 11 model are coupled with MIKE 21 in the MIKE FLOOD setup for the flood years 2001 and 2006; and flood inundation simulation is carried out.

5.1.1 MIKE 11 hydrodynamic model setup

After the model inputs are provided, calibration and validation of MIKE 11 model is carried out. During the process of calibration of MIKE 11 HD model, the Manning's roughness coefficients '*n*' of the river bed and banks are used as the calibration parameters. The values of roughness coefficient for the sluggish rivers are found to be in the range of 0.035–0.05 (Chow 1959). Initially, the setup was simulated using the Manning's roughness coefficient, *n* value as 0.05 for all the rivers. During calibration, the roughness coefficients are adjusted to obtain a close agreement between the observed and simulated discharges as well as water levels. The MIKE 11 model is calibrated using data for the period July 5, 2003, to October 30, 2003 (monsoon season). The simulated discharge values at all the four discharge gauging sites, viz. Balianta, Naraj, Cuttack and Tarapur and the simulated water levels at six gauging stations, viz. Naraj, Balianta, Cuttack, Tarapur, Nimapara and Alipingal are compared with the corresponding observed values. The simulated discharge and water level at all the river escapes, except Mancheswar escape, are also compared with the corresponding observed values. The process of adjusting '*n*' is continued until the observed and the simulated values at the gauging sites are in close agreement. Figures 3 and 4

Table 2 Details of different rice varieties

Type of rice variety	Name of variety	Grain yield (t/ha)	Duration (days)	Plant height (cm)	Flowering days
Normal	Swarna	4.5	160	85	112
Shallow	Sabita	4.2	160	90	114
Medium deep	Varshdhan	3.2	165	80–120	130
Deep water	Jalmagna	3.0	180	120–150	140
Submerged	Swarna Sub-1	4.4	160	90	120

present the comparison of the observed and simulated discharges/water levels at all the stations. Error function values obtained for these stations are shown in Tables 4, 5, 6 and 7. It is observed from Tables 4, 5, 6 and 7 that the index of agreement (d) for all the gauging locations are above 0.78, which suggests that the model calibration is acceptable. High coefficient of determination (R^2) values show that the simulated discharge values have good agreement with the trend of observed values. The RMSE values are quite small compared to the observed values. The percentage deviation in peak values for all the gauging site shows a good agreement between the observed and simulated peak discharge. Naraj gauging site has a close agreement between observed and simulated discharge throughout the simulation period. All other gauging sites show a good agreement between observed and simulated discharges during peak period only, whereas during non-peak periods there are differences. This difference is due to higher simulated discharge values as Naraj barrage on Kathajodi river head and Jobra barrage on Mahanadi river are not considered in the model setup. The peak flows are in good agreement because of negligible interference of the barrage regulations in flow conditions during the flood period. Due to unavailability of barrage regulation data, both Naraj and Jobra barrages are not considered in the model setup. The final values of the calibrated parameters, i.e., the global and local values of n are presented in Table 8.

To validate the calibrated model, the data for the monsoon period of the years 2002 (15th June–30th October) and 2004 (20th June–30th October) are used. The validation of the model is carried out for four discharge gauging stations and six water level gauging stations as in calibration. The error function values for the discharge and water level gauging stations for the years 2002 and 2004 are shown in Tables 9 and 10. From above tables, it is evident that the simulated discharges and water levels are found to be in reasonably close agreement with the corresponding observed values for the years 2002 and 2004. The deviation in peak is very low indicating the peak flow prediction is very close to that of observed. The values of error functions are as good as those obtained during calibration process. The model shows better prediction during high flow conditions. At these stations, the peak is preserved and the same reason mentioned earlier in the calibration section is responsible for the variation in observed and simulated discharge and stage values. The flows through escapes are found to be zero as the escapes are non-functional during 2002 and 2004. Thus, the performance of MIKE 11 model is found to be reasonably good during validation. This MIKE 11 setup is thus used for flood inundation simulation using MIKE FLOOD.

5.1.2 MIKE FLOOD model setup

MIKE 21 model setup is prepared prior to MIKE FLOOD model setup. MIKE 21 model setup requires three major input data sets, i.e., floodplain bathymetry in terms of elevation

Table 3 Relationship among depth-duration-damage for normal, shallow water, medium deep water and deep water rice variety

Normal rice variety			Shallow water rice variety			Medium deep water rice variety			Deep water rice variety		
Depth (m)	Duration of flood inundation (days)	Damage (%)	Depth (m)	Duration of flood inundation (days)	Damage (%)	Depth (m)	Duration of flood inundation (days)	Damage (%)	Depth (m)	Duration of flood inundation (days)	Damage (%)
0.1–0.5	8–21	100	>0.5	2–20	100	>1.0	2–20	100	>2.0	2–20	100
0.5–1.0	8–21	100	>0.5	0–1	80	>1.0	1–2	80	>2.0	0–1	80
>1.0	8–21	100	0.2–0.5	15–20	70	>1.0	0–1	15	1.0–2.0	7–25	28
>1.0	6–8	78	0.2–0.5	10–15	48	0.5–1.0	7–25	12	0.2–0.7	10–25	20
0.5–1.0	6–8	70	0.2–0.5	6–10	35	0.5–1.0	0–7	0	1.0–2.0	0–7	12
>1.0	5–6	64	0.2–0.5	4–6	28	0–0.5	0–25	0	0.7–1.0	0–25	6
>1.0	3–5	50	0.2–0.5	2–4	20				0.2–0.7	0–10	0
0.5–1.0	5–6	44	0.2–0.5	1–2	10				0–0.2	0–25	0
0.5–1.0	3–5	40	0.2–0.5	0–1	0						
0.1–0.5	6–8	38	0–0.2	0–21	0						
>1.0	1–2	36									
0.1–0.5	5–6	28									
0–0.5	3–5	24									
0.5–1.0	1–2	23									
>1.0	0–1	20									
0.1–0.5	1–2	18									
0.5–1.0	0–1	12									
0–0.1	0–25	0									

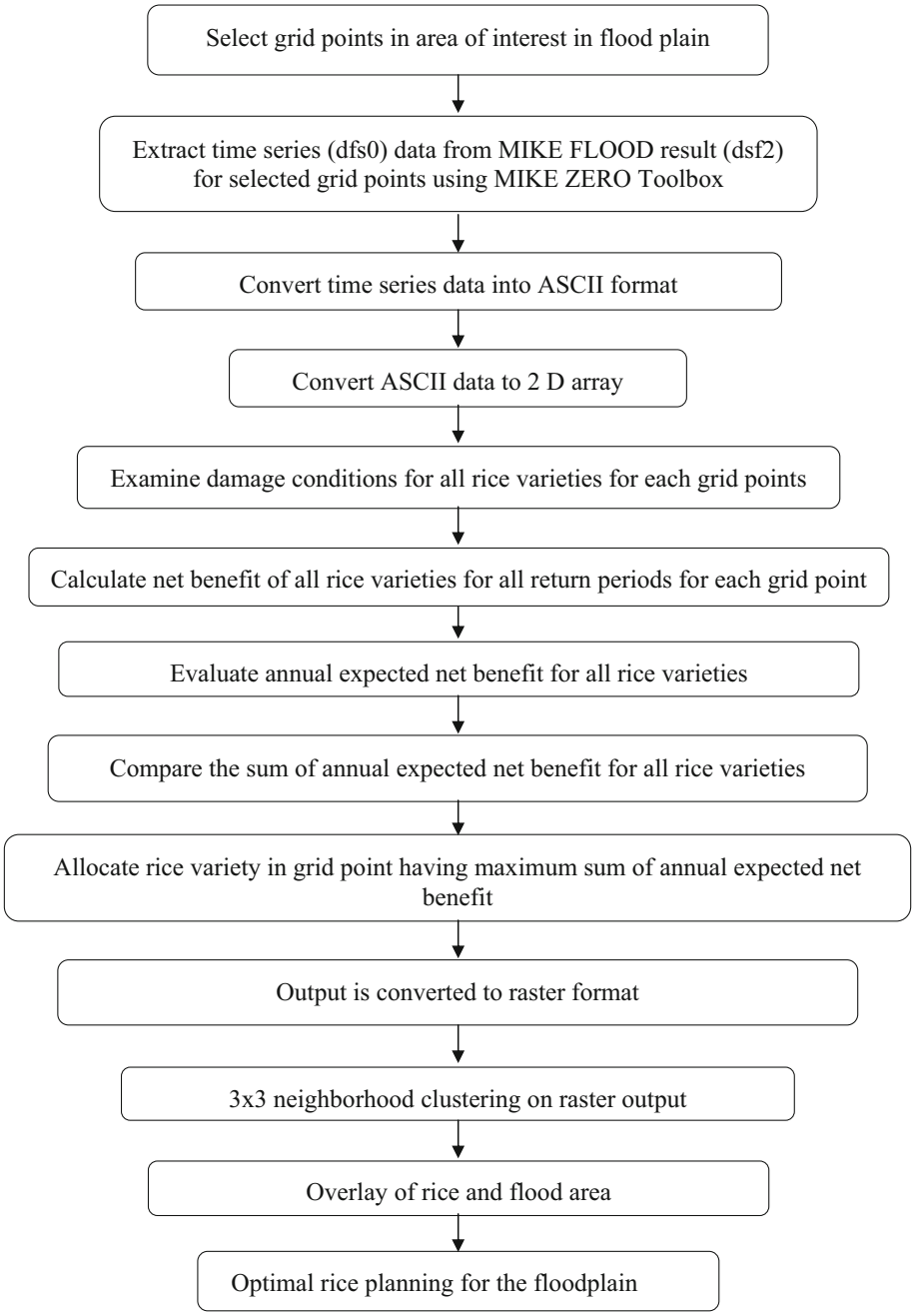

Fig. 2 Flowchart showing optimal rice planning procedure after extracting results from MIKE FLOOD

values; mean areal rainfall values; and roughness co-efficient values of the floodplain. The bathymetry file is prepared by using SRTM DEM. Rainfall file is prepared using Thiessen polygon method. The Thiessen weights for nine ordinary raingauge, i.e., Puri, Nimapara,

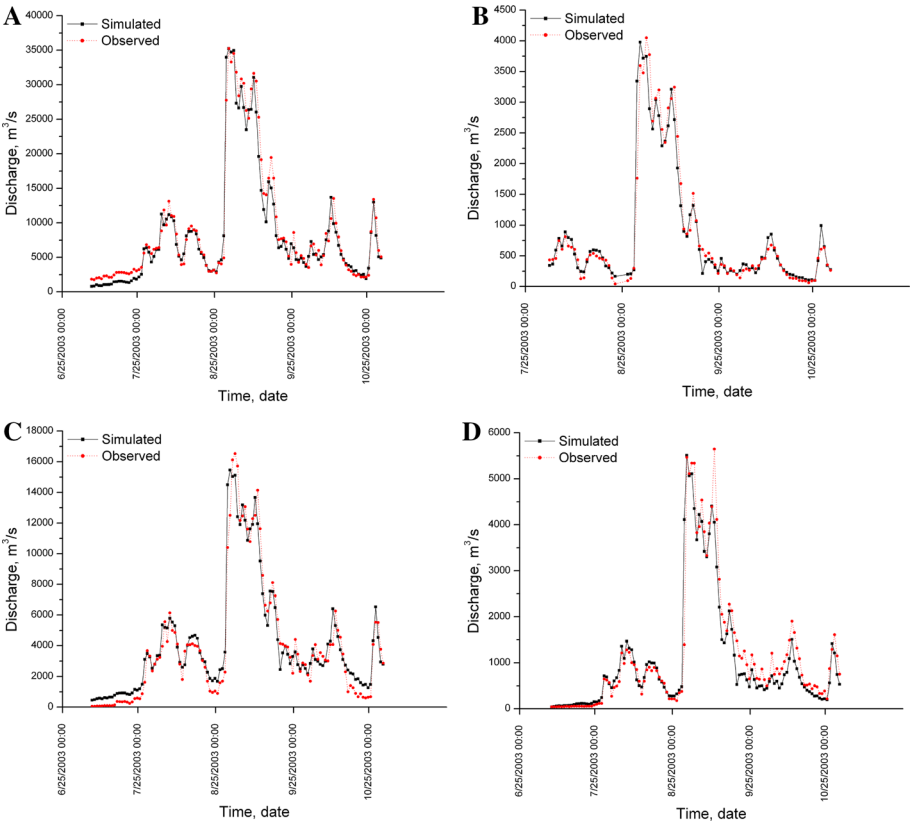

Fig. 3 Comparison of observed and simulated discharges at Naraj (**a**), Balianta (**b**), Cuttack (**c**) and Tarapur (**d**) during calibration for the year 2003

Bhubaneswar, Kakatpur, Barmul, Paradip, Kendrapara, Cuttack and Naraj stations are determined. Using these weights and station-wise rainfall values, the rainfall file is prepared. Most part of the study area is agricultural land; hence, according to Chow (1959), Manning's roughness co-efficient for the floodplain is fixed as 0.05.

For flood inundation mapping, MIKE FLOOD model setup is prepared using the calibrated MIKE 11 model and MIKE 21 model for the flooding years 2001 and 2006. MIKE FLOOD simulation is carried out during the peak discharge period, i.e., July 10 to August 2, 2001; and August 24 to September 16, 2006.

5.2 Flood inundation mapping using remote sensing data in GIS

The flood date RADARSAT-1 image is classified using histogram thresholding technique to delineate the flood-inundated areas. RADARSAT-1 images of July 20, 2001 and September 4, 2006 are used in this study. For RADARSAT imagery with HH polarization, flood water can have a backscatter value around −12 dB (Pandey 2009; Manjushree et al. 2012). From the histogram of RADARSAT imageries, it is observed that there is peak at

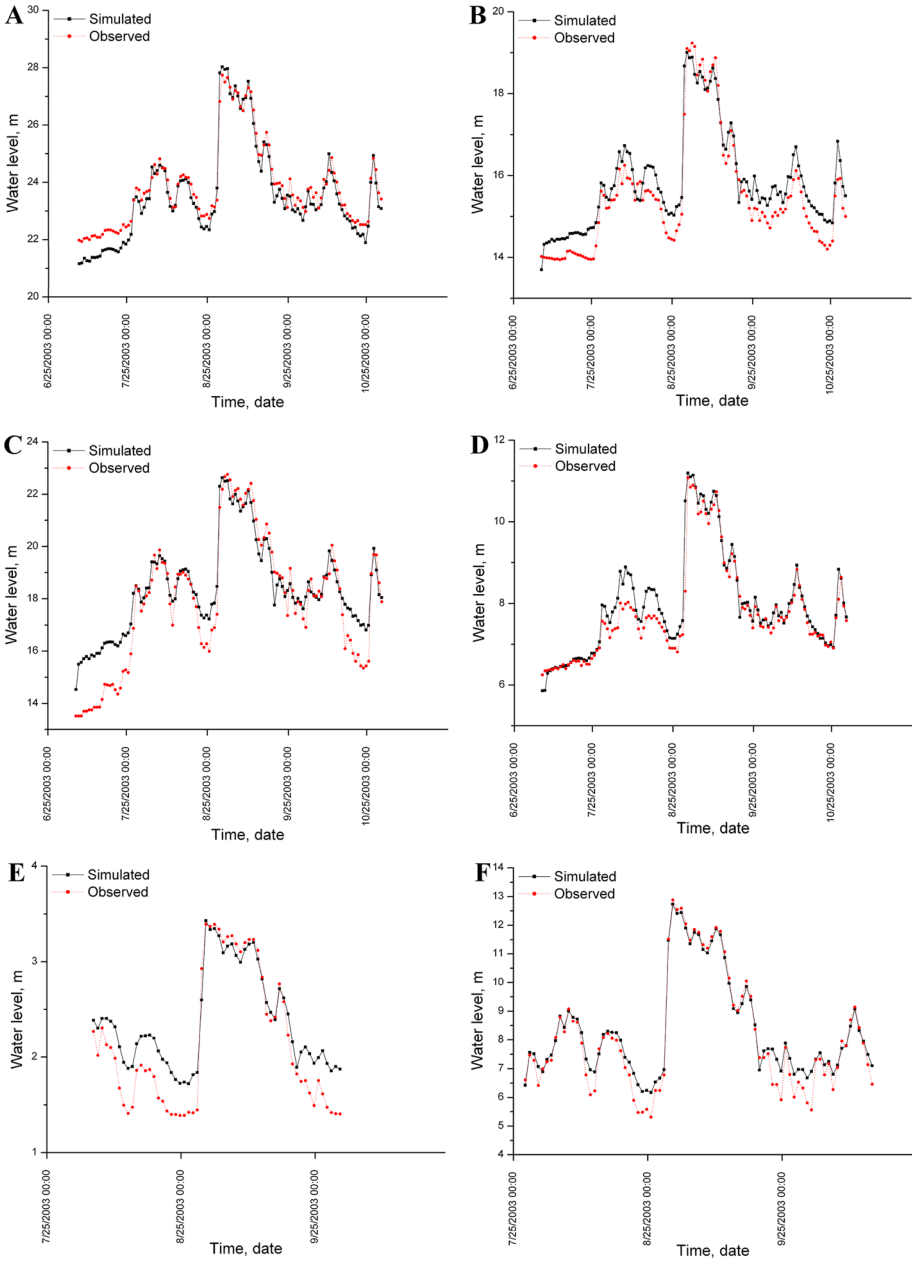

Fig. 4 Comparison of observed and simulated water levels at Naraj (**a**), Balianta (**b**), Cuttack (**c**), Tarapur (**d**), Nimapara (**e**) and Alipingal (**f**) during calibration for the year 2003

−12.9 dB for 2001 imagery and −13.2 dB for 2006 imagery. Therefore, −12.9 dB is used as threshold value for July 20, 2001 RADARSAT imagery and −13.2 dB is used as threshold value for that of September 4, 2006.

Table 4 Error function values for different discharge gauging stations during calibration for the year 2003

Error functions	Name of discharge gauging stations			
	Naraj	Balianta	Cuttack	Tarapur
RMSE (m^3/s)	1,769.80	247.33	966.41	405.75
MAE (m^3/s)	1,264.50	129.82	740.96	234.97
R^2	0.96	0.94	0.94	0.92
d	0.99	0.98	0.98	0.98
Absolute deviation in peak (m^3/s)	30.18	73.78	1,081.18	137.22
Percentage deviation in peak (%)	−0.09	−1.82	−6.54	−2.43

Table 5 Error function values for different water level gauging stations during calibration for the year 2003

Error functions	Name of water level gauging stations					
	Naraj	Balianta	Cuttack	Tarapur	Nimapara	Alipingal
RMSE (m)	0.43	0.49	1.00	0.37	0.31	0.43
MAE (m)	0.38	0.46	0.77	0.24	0.26	0.31
R^2	0.98	0.96	0.94	0.94	0.97	0.98
d	0.98	0.96	0.94	0.98	0.94	0.99
Absolute deviation in peak (m)	0.29	0.23	0.13	0.12	0.03	0.15
Percentage deviation in peak (%)	1.05	−1.21	−0.57	1.05	0.95	−1.13

Table 6 Error function values for water level at different escapes during calibration for the year 2003

Error functions	Name of the escapes				
	Madipur	Kanti	Jogisahi	Ramchandrapur	Achyutpur
RMSE (m)	0.08	0.20	0.21	0.24	0.06
MAE (m)	0.06	0.11	0.16	0.22	0.06
R^2	0.92	0.65	0.94	0.96	0.86
d	0.98	0.88	0.90	0.83	0.92
Absolute deviation in peak (m)	0.00	0.12	0.05	0.18	0.04
Percentage deviation in peak (%)	−0.02	1.09	−0.26	1.04	−0.95

A difficulty faced in flood area delineation is that the backscatter values of flood area are almost equal to that of transplanted rice field. Standing water in transplanted rice fields can be classified as flood. Generally, in most of the agricultural areas in the study area, transplantation is done before 15th July of a year. Hence, there is more chance of false classification of transplanted rice field as flooded area in flood date of year 2001, i.e., 20th July; whereas, in flood date of year 2006, i.e., 4th September chances of false classification will be minimum. Therefore, to derive the final flood map of the study area for July 20, 2001, both regular water areas and rice areas obtained from the logical operations (Sects. 4.2.1, 4.2.2) are excluded from the flood area found in threshold image; whereas, to

Table 7 Error function values for discharge through different escapes during calibration for the year 2003

Error functions	Name of the escapes				
	Madipur	Kanti	Jogisahi	Ramchandrapur	Achyutpur
RMSE (m^3/s)	4.06	22.92	22.79	7.93	15.39
MAE (m^3/s)	3.22	14.04	19.93	6.74	13.98
R^2	0.88	0.41	0.95	0.96	0.85
d	0.97	0.78	0.93	0.97	0.90
Absolute deviation in peak (m^3/s)	0.14	21.16	6.33	1.12	11.62
Percentage deviation in peak (%)	−0.32	26.09	3.78	1.23	−5.12

Table 8 Calibrated Manning's n for MIKE 11 setup during calibration for the year 2003

Rivers and their chainages (km)	Resistance number, n	
	Local resistance number	Global resistance number
Daya (0.00–56,042.00)	0.032	0.050
Kandal (0.00–21,402.98)	0.033	
Kuakhai-Bhargavi (0.00–8,541.86)	0.045	
Kuakhai-Bhargavi (8,541.86–26,624.30)	0.044	
Kuakhai-Bhargavi (26,624.31–38,299.30)	0.032	
Kuakhai-Bhargavi (38,299.30–129,540.00)	0.035	
Kushabhadra (0.00–27,402.00)	0.033	
Chitroptala (0.00–12,960.00)	0.045	
Main Mahanadi (0.00–3,781.40)	0.030	
Main Mahanadi (35157.63-115935.00)	0.031	
Serua (0.00–15,167.39)	0.040	
Biluakhai (0.00–12,696.34)	0.040	
Kathajodi-Devi (0.00–89,376.30)	0.032	
Paika (0.00–34,299.30)	0.045	

derive the final flood map of the study area for September 4, 2006, only regular water areas are excluded from the flood area found in threshold image.

5.3 Validation of inundation map prepared using MIKE FLOOD

In order to validate the MIKE FLOOD model, the simulated inundation maps are compared to that of inundation maps obtained using RADARSAT images. Figure 5 shows the comparison between MIKE FLOOD-simulated inundation area and RADARSAT image-based inundation area for years 2001 and 2006. Comparison of observed and simulated inundated areas and fit percentage for the years 2001 and 2006 are presented in Table 11. It is observed from Fig. 5 that there is a reasonable agreement in the pattern of flooding between the observed and simulated flood-inundated areas at most of the locations for both 2001 and 2006. In both the cases, inundated area in MIKE FLOOD is more than that of RADARSAT image-based inundated area near the point where Mahanadi river drains into Bay of Bengal. In this region, MIKE FLOOD-simulated inundation area is 1,125.74 km^2

Table 9 Error function values for different discharge gauging stations during validation for the years 2002 and 2004

		RMSE (m^3/s)	MAE (m^3/s)	R^2	d	Absolute deviation in peak (m^3/s)	Percentage deviation in peak (%)
Naraj	2002	613.32	420.96	0.99	0.99	789.59	−4.75
	2004	1051.00	566.92	0.95	0.98	978.54	−4.36
Balianta	2002	136.10	119.52	0.97	0.96	84.12	6.78
	2004	151.96	97.75	0.92	0.98	90.44	5.02
Cuttack	2002	655.82	501.54	0.92	0.97	157.31	2.08
	2004	710.62	501.83	0.91	0.97	363.16	3.73
Tarapur	2002	166.43	127.71	0.96	0.97	133.32	6.84
	2004	219.42	176.82	0.91	0.96	340.18	13.08

Table 10 Error function values for different water level gauging stations during validation for the years 2002 and 2004

		RMSE (m)	MAE (m)	R^2	d	Absolute deviation in peak (m)	Percentage deviation in peak (%)
Naraj	2002	0.65	0.62	0.92	0.87	0.15	−0.58
	2004	0.62	0.59	0.97	0.92	0.02	0.08
Balianta	2002	0.25	0.19	0.97	0.98	0.23	1.37
	2004	0.33	0.24	0.93	0.96	0.32	1.83
Cuttack	2002	1.18	1.06	0.93	0.88	0.34	−1.64
	2004	1.26	1.13	0.94	0.87	0.01	0.02
Tarapur	2002	0.40	0.28	0.86	0.91	0.23	2.55
	2004	0.26	0.18	0.94	0.97	0.43	4.46
Nimapara	2002	0.15	0.14	0.99	0.97	0.04	1.58
	2004	0.31	0.28	0.82	0.84	0.13	4.35
Alipingal	2002	0.63	0.53	0.98	0.95	0.30	−2.97
	2004	1.43	1.25	0.94	0.85	0.11	0.99

for the year 2001 and 1,049.62 km^2 for the year 2006; whereas, RADARSAT image-based inundation areas are 327.04 km^2 for the year 2001 and 611.87 km^2 for the year 2006. In reality, Mahanadi river branches into several streams just before draining into Bay of Bengal, which reduces the flow in the main river. Thus, in flooding conditions, less water from Mahanadi river spills out to the floodplain. In MIKE FLOOD model setup, only Mahanadi river is included without considering the small branches near the draining point; thus, the simulated flow is on the higher side. Hence, in MIKE FLOOD model, more flow is spilled out to the floodplain generating higher inundated areas. In both 2001 and 2006, inundated area in MIKE FLOOD is less than that of RADARSAT image-based inundated area in the downstream areas of Kushabhadra, Daya and Bhargabi. In this region, MIKE FLOOD-simulated inundation areas are 681.34 km^2 for the year 2001 and 615.83 km^2 for the year 2006; whereas, RADARSAT image-based inundation areas are 1,113.92 km^2 for the year 2001 and 957.42 km^2 for the year 2006. In this region, the major reasons of flooding are presence of escapes, canal breaching and river embankment breaching. Hence,

MIKE FLOOD-inundated area in this region is less as canal and river embankment breaching are not considered in the model setup. However, 45 % of inundated area of RADARSAT image is well simulated by MIKE FLOOD model while the %fit is 24.95 % for year 2001. Similarly, for year 2006, around 52 % of inundated area of RADARSAT image is well simulated by MIKE FLOOD model while %fit is 33.90.

5.4 L-moment-based flood frequency analysis

L-moment-based at-site flood frequency analysis is carried out at Naraj gauging site as it is at the upstream end of the present study area. Fifty-four years peak discharge data from the years 1955–2008 are used for frequency analysis. Various distributions namely Generalized logistic distribution (GLO), Generalized extreme-value distribution (GEV), Generalized Normal (lognormal) distribution (GN), Pearson type III distribution (PE3), Generalized Pareto distribution (GPA) and Wakeby distribution (WAK) are used. L-moment ratio diagram is plotted (Fig. 6) and Z^{dist} for each distribution is calculated. The Z-values for GLO, GEV, GN, PE3 and GPA are found to be 1.84, 2.88, 2.69, 2.72 and 4.85, respectively. In the present study, Wakeby distribution is identified as the robust distribution for the Naraj gauging site as no other distribution has Z^{dist} value lower than 1.64, which is the basis for selecting the distribution. The parameters of the Wakeby distribution are estimated as: $\zeta = 0.085$; $\beta = 6.399$; $\alpha = 9.354$; $\gamma = 0.306$; and $\delta = -0.029$. Growth factors for different return periods are calculated using the distribution. For the estimation of floods of various return periods for the study area, the mean annual peak flood at Naraj site is multiplied by corresponding values of the growth factor. The mean discharge of the Naraj site from available 54-year data is 23,827 m^3/s. For 100 year return period, the flood discharge at Naraj is calculated as 49,751 m^3/s.

5.5 Flood hazard mapping using MIKE FLOOD

As discussed in previous section, at-site flood frequency analysis is carried out to estimate the flood peaks of return periods 2, 10, 25, 50, 100 and 200 years for Naraj gauging site which is the upstream boundary of the flood inundation model. The flood hydrograph shape is obtained by analyzing the peak flood hydrographs that occurred during each of the four years at Naraj gauging site: 2001, 2003, 2006 and 2008.

Figure 7 shows a plot of the peak flood hydrographs (hourly discharge values) for each of the four years, i.e., 2001, 2003, 2006 and 2008 for Naraj gauging site. From Fig. 7, it is observed that the flood event of the year 2008 has the highest peak while that of 2006 has the lowest peak. In a non-dimensional analysis, the peaks of these hydrographs are scaled to a constant ordinate value of 1 by dividing discharge ordinates of each year by the corresponding peak discharge of the same year. From Fig. 7, it is observed that the widest hydrograph for the Naraj site is that of the year 2001.

Thus, the flood scenario hydrographs are constructed by selecting the widest hydrograph considering the upper portion of the flood wave that is responsible for causing flood inundation. The widest hydrograph is considered because it is expected to cause the worst flood. Subsequently, each discharge ordinate of the widest hydrograph is multiplied by an amplifier, which is the flood corresponding to 100-year return period for Naraj gauging site. This transformation yields the widest flood hydrograph corresponding to 100 year return period for Naraj gauging site. This procedure is similar to the one used by Forster et al. (2008a).

Using the 100-year return period flood hydrograph as input to the MIKE 11 model, model simulation is carried out. Subsequently, MIKE FLOOD simulation is carried out for obtaining the 100-year return period flood inundation as shown in Fig. 8.

5.6 Optimal rice planning for the study area

Optimal rice planning is carried out on the basis of sum of average annual expected net benefit (INR/ha) for 5-, 10-, 25-, 50- and 100-year return period floods for normal, shallow, medium deep and deep water rice varieties. The entire area is divided into grids of size 528×528 m^2, as per the MIKE FLOOD model setup. For annual expected net benefit, probability of flooding is obtained from the flood frequency analysis and vulnerability of the crops to damage estimated from the depth-duration-damage functions for different rice varieties. A program in C programming language is developed to evaluate expected annual net benefit from the stage-duration-damage function for different rice varieties on the basis of flood depth-duration series obtained from MIKE FLOOD for all the grids in the study area. To allocate a particular rice variety in a grid, the sum of average annual expected net benefit for different return period floods is calculated for each variety individually and the variety with maximum sum is allocated to that particular grid.

The procedure followed for allocation of rice variety in a particular grid is described hereafter:

From a survey following information are obtained:

Average market price of rice = 9.50 INR/kg
Average seed rate of rice = 60 kg/ha
Average seed price of rice = 20 INR/kg

To estimate the recovery factor for a rice variety in a grid, the stage-duration series data are extracted from MIKE FLOOD result for each specified return period and tested against the conditions specified in Table 3. Computation of average expected net benefit for normal rice variety for a particular grid is shown in Table 12.

The sample computations for 25-year return period are given below:

$$\begin{aligned}\text{Net benefit} &= \text{yield (kg/ha)} \times \text{recovery factor} \times \text{market price (INR/kg)} \\ &\quad - \text{average cultivation cost (INR/ha)} \\ &\quad - \text{seed rate (kg/ha)} \times \text{seed cost(INR/kg)} \\ &= 4500 \times 0.78 \times 9.50 - 15000 - 60 \times 20 \\ &= 17145 \text{ INR/ha} = 477831.15 \text{ INR/grid}\end{aligned}$$

$$\begin{aligned}\text{Annual extreme probability} &= (\text{return period})^{-1} \\ &= (25)^{-1} \\ &= 0.04\end{aligned}$$

$$\begin{aligned}\text{Interval probability} &= \text{annual extreme probability of previous return period} \\ &\quad - \text{annual extremeprobability of calculating return period} \\ &= 0.10 - 0.04 = 0.06\end{aligned}$$

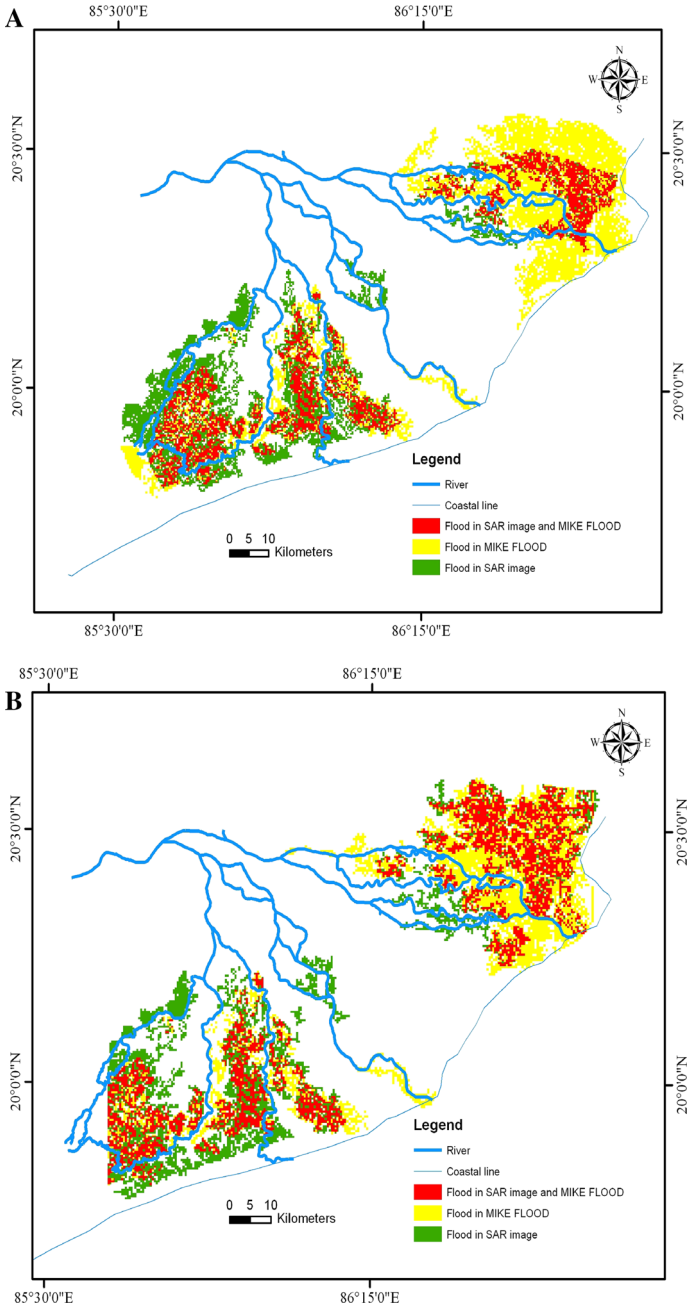

Fig. 5 Overlaid flood inundation maps obtained from SAR and MIKE FLOOD for 20th July 2001 (**a**) and 04th September 2006 (**b**)

Table 11 Fit percentage for MIKE FLOOD inundation area with RADARSAT image-based inundation area for the years 2001 and 2006

Date		20/07/2001	04/09/2006
Flood-inundated area	MIKE FLOOD (IA_{mod}) (km^2)	1,807.08	1,665.45
	RADARSAT image (IA_{obs}) (km^2)	1,440.96	1,569.29
Parameters fit measure	$IA_{obs} \cap IA_{mod}$ (km^2)	648.75	819.06
	IA_{obs} U IA_{mod} (km^2)	2,599.28	2,415.68
	Fit (%)	24.95	33.90

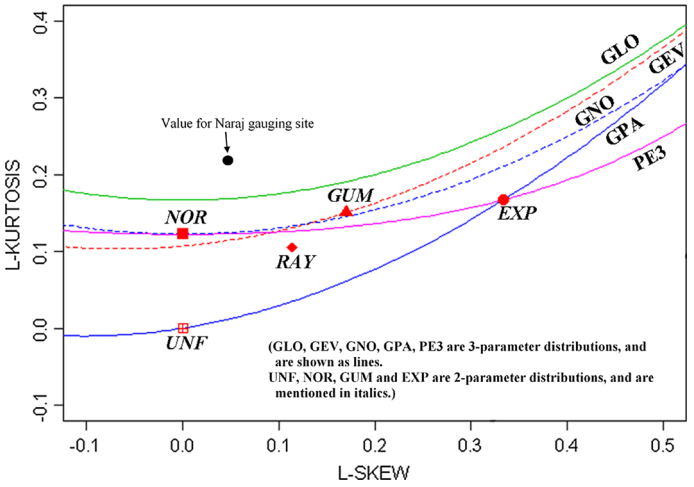

Fig. 6 L-moment ratio diagram for Naraj gauging site of Mahanadi river basin

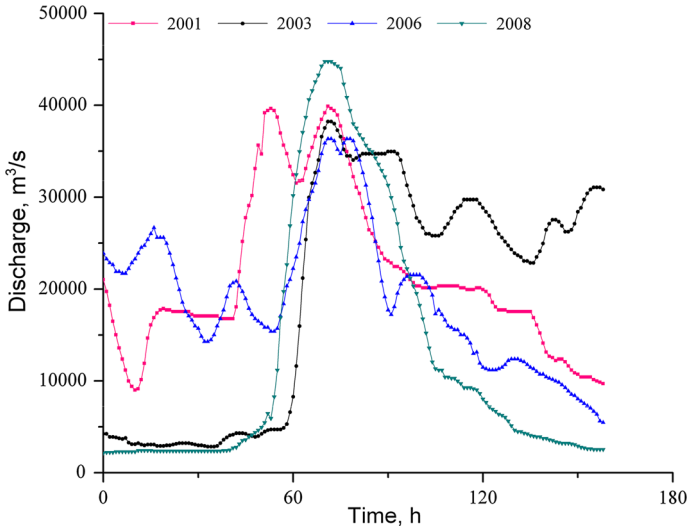

Fig. 7 Peak flood hydrographs of Naraj gauging site for the years 2001, 2003, 2006 and 2008

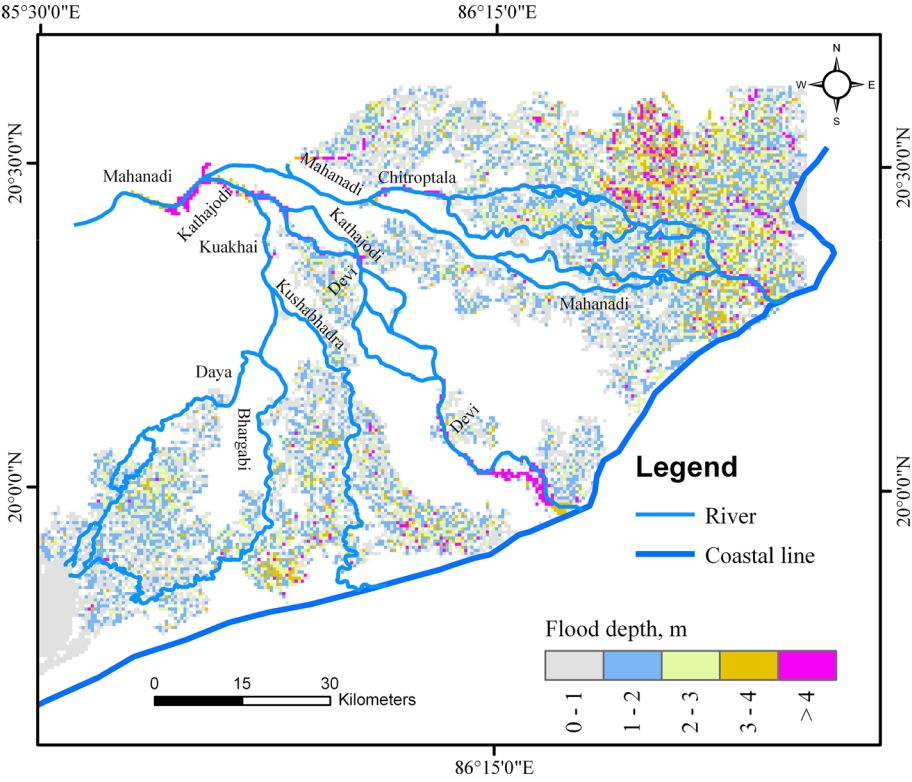

Fig. 8 Maximum flood depth map of 100 year return period flood obtained using MIKE FLOOD

Table 12 Average annual expected net benefit for normal rice variety at a particular grid

Return Period, year	Annual extreme probability	Net benefit, INR/grid	Interval probability	Interval average net benefit, INR/grid	Average Annual expected net benefit, INR/grid
5	0.20	739,948.50			
10	0.10	680,376.38	0.10	710,162.44	71,016.24
25	0.04	477,831.15	0.06	579,103.76	34,746.22
50	0.02	382,515.75	0.02	430,173.45	8,603.47
100	0.01	85,714.18	0.01	234,114.96	2,341.14
				Total	116,707.07

$$\begin{aligned}\text{Interval average net benefit} &= (\text{net benefit of previous return period} \\ &\quad + \text{ net benefit of calculating return year})/2 \\ &= (680376.38 + 477831.15)/2 \\ &= 579103.76 \text{ INR/grid}\end{aligned}$$

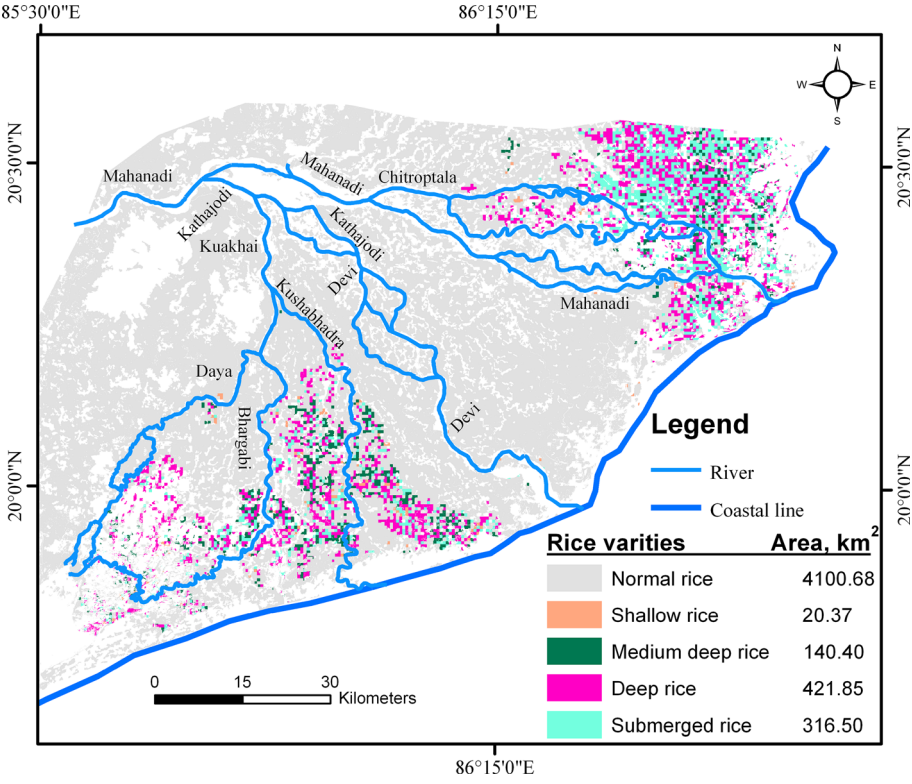

Fig. 9 Optimal allocation of rice varieties for the delta region of Mahanadi river basin considering flood risk

$$\begin{aligned}\text{Average annual expected net benefit} &= \text{interval average net benefit} \\ &\quad \times \text{annual extreme probability} \\ &= 579103.76 \times 0.06 = 34746.22 \text{ INR/grid}\end{aligned}$$

Comparison is carried out among sum of average annual expected net benefit for all rice varieties. Subsequently, rice variety having highest sum of average annual net benefit is allocated to the grid.

The above stated operation is executed for each grid through the C program which generates an ASCII file with crop allocation for the study area on grid basis. The output of the C program is transferred to GIS platform as an image file with each grid specified with the allocated rice variety. Figure 9 shows optimal allocation of rice varieties for the study area.

The sum of average annual expected net benefit of optimal crop allocation model corresponding to all the specified return period floods for the study area is INR 601.054 million. In case only normal rice variety is cultivated throughout the study area, the sum of average annual expected net benefit is INR 431.509 million. Similarly, in case only shallow rice, medium deep and deep water rice varieties are cultivated throughout the study area, the sum of average annual expected net benefits are INR 341.386 million, INR

259.378 million and INR 240.001 million, respectively. Hence, it is observed that in the long run, the net benefit from the optimal allocation of rice varieties model is maximum.

6 Conclusions

The present study concludes that SRTM DEM may be used for extraction of acceptable topographic data in large flood-prone regions where high-resolution DEM is not available. MIKE 11 model setup using SRTM DEM-derived cross sections simulates river stage and discharge data quite satisfactorily in the present study. The MIKE FLOOD-simulated flood inundation pattern in the study area, i.e., delta region of Mahanadi river basin is in reasonable agreement with the observed pattern of flood inundation obtained from RADARSAT-1 images. Flood hazard maps obtained from MIKE FLOOD model along with the flood vulnerability data for different rice varieties are used to develop an optimal rice allocation model for the study area. Optimal rice allocation model prepared for the study area gives the maximum average annual expected net benefit considering the flood risk in the region. The sum of average annual expected net benefit of optimal rice allocation model for the study area is to the tune of INR 601.054 million; whereas, in case of only normal rice variety cultivation throughout the study area, the sum of average annual expected net benefit is INR 431.509 million. The obtained results are subjected to certain limitations due to omission of drainage and canal networks in MIKE 11 model, not considering the river breaching points in preparing the hazard maps and assumptions made in the optimal crop allocation model development. This study demonstrates a unique methodology for optimal rice planning in flood-prone regions considering the flood risk involved.

Acknowledgments This study has been done as a part of a project titled "Flood Risk Modeling Using Satellite Remote Sensing Data for Optimal Crop Planning", sponsored by Indian Space Research Organization (ISRO), Bangalore. The authors also acknowledge the help of Mr. Natkar Suraj Rajaram, a former postgraduate student of Indian Institute of Technology, Kharagpur.

References

Aronica G, Bates PD, Horritt MS (2002) Assessing the uncertainty in distributed model predictions using observed binary pattern information within GLUE. Hydrol Process 16:2001–2016

Bates PD, De Roo APJ (2000) A simple raster based model for flood inundation simulation. J Hydrol 236:54–77

Bates PD, Marks KJ, Horritt MS (2003) Optimal use of high-resolution topographic data in flood inundation models. Hydrol Process 17:537–557

Bazi Y, Bruzzone L, Melgani F (2005) An unsupervised approach based on the generalized Gaussian model to automatic change detection in multitemporal SAR images. IEEE Trans Geosci Remote Sens 43:874–887

Bouwer LM, Bubeck P, Wagtendonk AJ, Aerts JCJH (2009) Inundation scenarios for flood damage evaluation in polder areas. Nat Hazards Earth Syst Sci 9:1995–2007

Buchele B, Kreibich H, Kron A, Thieken A, Ihringer J, Oberle P (2006) Flood-risk mapping: contributions towards an enhanced assessment of extreme events and associated risks. Nat Hazards Earth Syst Sci 6:485–503

Burrel BC, Davar K, Hughes R (2007) A review of flood management considering the impacts of climate change. Water Int 32(3):342–359

Central Water Commission (CWC) (2010) Water and Related Statistics. CWC, New Delhi

Chaoudhury I, Chakraborty M (2006) SAR signature investigation of rice crop using RADARSAT data. Int J Remote Sens 27(3):519–534

Chatterjee C, Forster S, Bronstert A (2008) Comparison of hydrodynamic models of different complexities to model floods with emergency storage areas. Hydrol Process 22:4695–4709
Chow VT (1959) Open-channel hydraulics. McGraw-Hill Book Company, New York
Dang NM, Babel MS, Luong HT (2011) Evaluation of flood risk parameters in the Day river flood diversion area, Red river delta, Vietnam. Nat Hazards 56:169–194
DHI (2004) MIKEFLOOD 1D-2D modelling user manual. Danish Hydraulic Institute, Horsholm
Di Baldassarre G, Schumann G, Bates P (2009) Near real time satellite imagery to support and verify timely flood modelling. Hydrol Process 23:799–803
Dutta D, Herath S, Musiake K (2003) A mathematical model for flood loss estimation. J Hydrol 277:24–49
Forster S, Chatterjee C, Bronstert A (2008a) Hydrodynamic simulation of the operational management of a proposed flood emergency storage area at the middle Elbe river. River Res Appl 24:900–913
Forster S, Kuhlmann B, Lindenschmidt KE, Bronstert A (2008b) Assessing flood risk for a rural detention area. Nat Hazards Earth Syst Sci 8:311–322
Haile AT, Rientjes THM (2005) Effects of DEM LIDAR resolution in flood modeling: a model sensitivity study for the city of Tegucigalpa, Honduras. In: ISPRS workshop 'Laser Scanning 2005' Enschede the Netherlands September 12–14, pp 168–173
Hoes O, Schuurmans W (2006) Flood standards or risk analyses for polder management in the Netherlands. Irrig Drain 55:S113–S119
Horritt MS (2006) A methodology for the validation of uncertain flood inundation models. J Hydrol 326(1–4):153–165
Hosking JRM (1990) L-moments: analysis and estimation of distributions using linear combinations of order statistics. J R Stat Soc Ser B Methodol 52:105–124
Kazama S, Sato A, Kawagoe S (2009) Evaluating the cost of flood damage based on changes in extreme rainfall in Japan. Sustain Sci 4:61–69
Khan SI, Hong Y, Wang J, Yilmaz KK, Gourley JJ, Adler RF, Brakenridge GR, Policelli F, Habib S, Irwin D (2011) Satellite remote sensing and hydrologic modeling for flood inundation mapping in Lake Victoria basin: implications for hydrologic prediction in ungaged basins. IEEE Trans Geosci Remote Sens 49(1):85–95
Khatua KK, Patra KC (2004) Management of high flood in Mahanadi and its tributaries below Naraj. In: 49th annual session of IEI (India) Bhubaneswar Orissa
Kjelds J, Rungo M (2002) Dam breach modeling and inundation mapping. Danish Hydraulic Institute Denmark
Kumar R, Chatterjee C (2005) Regional flood frequency analysis using L-moments for North Brahmaputra region of India. J Hydrol Eng Am Soc Civil Eng 10(1):1–7
Long NT, Trong BD (2001) Flood monitoring of Mekong River Delta Vietnam using ERS SAR Data. In: 22nd Asian conference of remote sensing, Singapore
Luino F, Cirio CG, Biddoccu M, Agangi A, Giulietto W, Godone F, Nigrelli G (2009) Application of a model to the evaluation of flood damage. Geoinformatica 13:339–353
Mani P, Chatterjee C, Kumar R (2014) Flood hazard assessment with multiparameter approach derived from coupled 1D and 2D hydrodynamic flow model. Nat Hazards 70:1553–1574
Manjushree P, Kumar LP, Bhatt CM, Rao GS, Bhanumurthy V (2012) Optimization of threshold ranges for rapid flood inundation mapping by evaluating backscatter profiles of high incidence angle SAR images. Int J Disaster Risk Sci 3(2):113–122
Matgen P, Hostache R, Schumann G, Pfister L, Hoffmann L, Savenjie HHG (2011) Towards an automated SAR-based flood monitoring system: lessons learned from two case studies. Phys Chem Earth 36:241–252
Mileti DS (1999) Disasters by design: a reassessment of natural hazards in the United States. Joseph Henry, Washington
NDMA (2008) National disaster management guidelines: management of floods. National Disaster Management Authority, Government of India, New Delhi
Nicholas AP, Walling DE (1997) Modelling flood hydraulics and overbank deposition on river floodplains. Earth Surf Process Landf 22:59–77
Pandey A (2009) Mapping of 2006 flood extent in Birupa basin, Orissa, India, using visual and digital classification techniques on RADARSAT image: a comparative analysis. Published thesis. International Institute for Geo-information Science and Earth Observation Enschede, The Netherlands
Parhi PK, Mishra SK, Singh R, Tripathi VK (2012) Floods in Mahanadi river basin Orissa (India): a critical review. India Water Week-Water Energy and Food Security
Patro S, Chatterjee C, Mohanty S, Singh R, Raghuwanshi N (2009a) Flood inundation modeling using MIKE FLOOD and remote sensing data. J Indian Soc Remote Sens 37:107–118

Patro S, Chatterjee C, Singh R, Raghuwanshi N (2009b) Hydrodynamic modelling of a large flood-prone river system in India with limited data. Hydrol Process 23(19):2774–2791
Penning-Rowsell E, Tunstall S (1996) Risks and resources: defining and managing the floodplain. Floodplain processes, chap 15, Wiley, London, pp 493–533
Pramanik N, Panda R, Sen D (2010) One dimensional hydrodynamic modeling of river flow using DEM extracted river cross-sections. Water Resour Manag 24:835–852
Progress Report Vol 1: Varietal Improvement (2008) All india coordinated rice improvement programme, directorate of rice research, ICAR, Rajendranagar Hyderabad Aandra Pradesh
Rungo M, Olesen KW (2003) Combined 1- and 2- dimensional flood modeling 4th Iranian hydraulic conference 21–23 Oct, Shiraz, Iran
Sanders BF (2007) Evaluation of on-line DEMs for flood inundation modeling. Water Resour 30:1831–1843
Sanyal J, Lu XX (2004) Application of remote sensing in flood management with special reference to monsoon Asia: a review. Nat Hazards 33:283–301
Schumann G, Bates PD, Horritt MS, Matgen P, Pappanberger F (2009) Progress in integration of remote sensing derived flood extent and stage data and hydraulic models. Rev Geophys 47:RG4001
Schumann G, Di Baldassarre G, Alsdorf D, Bates PD (2010) Near real time flood wave approximation on large rivers from space: application to the river Po, Italy. Water Resour Res 46:W05601
Shuttle breeding network project final report (2008) Orissa University of Agriculture and Technology, Orissa
SRC (2008–09) Special relief commission: annual report, Orissa
SRC (2011–12) Special relief commission: annual report, Orissa
Tarekegn TH, Haile AT, Rientjes T, Reggiani P, Alkema D (2010) Assessment of an ASTER-generated DEM for 2D hydrodynamic flood modeling. Int J Appl Earth Obs Geoinform 12:457–465
Thieken AH, Ackermann V, Elmer F, Kreibich H, Kuhlmann B, Kunert U, Maiwald H, Merz B, Müller M, Piroth K, Schwarz J, Schwarze R, Seifert I, Seifert J (2008) Methods for the evaluation of direct and indirect flood losses. In: 4th international symposium on flood defence, Institute for Catstophic Loss Reduction, Canada 98:1–10
UNFCCC (2007) Climate change: impacts, vulnerabilities and adaptation in developing countries. United Nations Framework Convention on Climate Change, Bonn
Vanderkimpen P, Melger E, Peeters P (2009) Flood modeling for risk evaluation—a MIKE FLOOD vs SOBEK 1D2D benchmark study. In: Flood risk management: research and practice. Taylor & Francis, London, pp 77–84
Villanueva I, Wright NG (2006) Linking Riemann and storage cell models for flood prediction. Inst Civil Eng Water Manag Proc 159:27–33
Waisurasingha C, Aniya M, Hirano A, Sommut W (2008) Use of RADARSAT-1 data and a digital elevation model to assess flood damage and improve rice production in the lower part of the Chi River Basin, Thailand. Int J Remote Sens 29(20):5837–5850
Wang W, Yang X, Yao T (2012) Evaluation of ASTER GDEM and SRTM and their suitability in hydraulic modelling of a glacial lake outburst flood in southeast Tibet. Hydrol Process 26:213–225
Werner MGF (2004) A comparison of flood extent modeling approaches through constraining uncertainties on gauge data. Hydrol Earth Syst Sci 8(6):1141–1152
Yang T, Xu CY, Shao QX (2010) Regional flood frequency and spatial patterns analysis in the Pearl River Delta region using L-moments approach. Stoch Environ Res Risk Assess 24:165–182